European Heart Journal – Cardiovascular Imaging (2014) **15**, 1333–1343
doi:10.1093/ehjci/jeu123

Patients with repaired tetralogy of Fallot suffer from intra- and inter-ventricular cardiac dyssynchrony: a cardiac magnetic resonance study

Linyuan Jing[1], Christopher M. Haggerty[1], Jonathan D. Suever[1], Sudad Alhadad[1], Ashwin Prakash[2,3], Frank Cecchin[2,3], Oskar Skrinjar[4], Tal Geva[2,3], Andrew J. Powell[2,3], and Brandon K. Fornwalt[1]*

[1]Departments of Pediatrics, Physiology, Biomedical Engineering and Medicine, University of Kentucky, UK Chandler Hospital, 741 S Limestone, BBSRB B353, Lexington, KY 40536, USA; [2]Department of Cardiology, Boston Children's Hospital, Boston, MA, USA; [3]Department of Pediatrics, Harvard Medical School, Boston, MA, USA; and [4]Scientific Imaging and Visualization LLC, Atlanta, GA, USA

Received 3 April 2014; accepted after revision 29 May 2014; online publish-ahead-of-print 4 July 2014

Aims Patients with repaired tetralogy of Fallot (rTOF) frequently have right bundle branch block. To better understand the contribution of cardiac dyssynchrony to dysfunction, we developed a method to quantify left (LV), right (RV), and inter-ventricular dyssynchrony using standard cine cardiac magnetic resonance (CMR).

Methods and results Thirty patients with rTOF and 17 healthy controls underwent cine CMR. Patients were imaged twice to assess inter-test reproducibility. Circumferential strain curves were generated with a custom feature-tracking algorithm for 12 LV and 12 RV segments in each of 4–7 short-axis slices encompassing the ventricles. Temporal offsets (TOs, in ms) of the strain curves relative to a patient-specific reference curve were calculated. The intra-ventricular dyssynchrony index (DI) for each ventricle was computed as the standard deviation of the TOs. The inter-ventricular DI was calculated as the difference in median RV and median LV TOs. Compared with controls, patients had a greater LV DI (21 ± 8 vs. 11 ± 5 ms, $P < 0.001$) and RV DI (60 ± 19 vs. 47 ± 17 ms, $P = 0.02$). RV contraction was globally delayed in patients, resulting in a greater inter-ventricular DI with the RV contracting 45 ± 25 ms later than the LV vs. 12 ± 29 ms earlier in controls ($P < 0.001$). Inter-test reproducibility was moderate with all coefficients of variation $\leq$22%. Both LV and RV DIs were correlated with measures of LV, but not RV, function.

Conclusion Patients with rTOF have intra- and inter-ventricular dyssynchrony, which can be quantified from standard cine CMR. This new approach can potentially help determine the contribution of dyssynchrony to ventricular dysfunction in future studies.

Keywords Dyssynchrony • Magnetic resonance imaging • Tetralogy of Fallot • Cardiac magnetic resonance

Introduction

Tetralogy of Fallot (TOF) is the most common cyanotic congenital heart disease with a prevalence of 356 per million live births.[1] The mortality rate of patients with TOF more than triples 25 years after their initial corrective surgery.[2] Two-thirds of this premature death are due to cardiac causes.[2] Thus, a critical barrier to extending life in patients with repaired TOF (rTOF) is identifying the underlying mechanisms of late cardiac failure.

Due to the high prevalence of right bundle branch block (RBBB) in patients with rTOF,[3] cardiac dyssynchrony may represent an important therapeutic target for use of cardiac resynchronization therapy to reduce mortality. A significant body of evidence has shown that left ventricular (LV) dyssynchrony not only leads to adverse remodelling in the LV,[4] but can also affect remodelling and synchrony in the right ventricle (RV).[5] Based on these studies, it is logical to question whether RV failure and RBBB cause similar detrimental effects in both ventricles in patients with rTOF.

* Corresponding author. Tel: +1 859 323 3243; Fax: +1 859 323 3499, E-mail: bkf@gatech.edu, b.f@uky.edu

The gold standard for imaging the RV is cine cardiac magnetic resonance (CMR), yet no technique has been developed to quantify left, right, and inter-ventricular dyssynchrony from standard cine CMR. We aimed to comprehensively evaluate dyssynchrony using a custom feature-tracking algorithm applied to routine cine CMR in healthy controls and patients with rTOF. We hypothesized that (i) cine CMR can be used to quantify dyssynchrony in both ventricles with good inter-test reproducibility in patients with rTOF and (ii) patients with rTOF suffer from intra- and inter-ventricular cardiac dyssynchrony likely due to RBBB.

Methods

Study subjects

Thirty patients with rTOF and 17 healthy controls were prospectively enrolled. Consecutive patients undergoing routine CMR were approached and informed about the study. Exclusion criteria included: (i) CMR under sedation and/or anaesthesia or (ii) significant imaging artefact due to ferromagnetic implant or cardiac arrhythmia. Approximately 30–40% of the patients approached were consented for the study. Controls had no history of cardiac disease, a normal 12-lead electrocardiogram (ECG), and a normal CMR. This study was approved by the Institutional Review Board.

Image acquisition

CMR images were obtained with either a 1.5-T Philips Achieva or Intera scanner with a 32-element phased-array cardiac coil (Philips Medical Systems, Best, the Netherlands). ECG-gated steady-state free precession (SSFP) short-axis images were acquired during 10–15 s breath holds with 20–30 image frames per cardiac cycle (reconstructed from 16 to 30 frames). Acquisition parameters were: matrix = 256 × 256, field of view = 280–400 mm, flip angle = 45–65°, repetition time (TR) = 2.8–4 ms, echo time (TE) = 1.5–2 ms, slice thickness = 8–10 mm, and slice gap = 0–2 mm. Two- and four-chamber SSFP long-axis cines were also acquired. To assess inter-test reproducibility, patients were imaged twice on the same day by different technologists.

Calculation of volumes, mass, and ejection fractions

Epicardial and endocardial boundaries at the end-diastolic frame were manually traced. LV and RV end-diastolic volume (EDV), end-systolic volume (ESV), stroke volume (SV), ejection fraction (EF), and myocardial mass were calculated as previously described.[6]

Displacement-based feature tracking

CMR images were analysed by a well-trained research assistant supervised by B.K.F. In each subject, the mitral and tricuspid valves were identified from end-systolic long-axis images, and all short-axis images located between the apex and the valve plane were selected for processing for both ventricles (*Figure 1A*). The number of slices analysed for each subject ranged from 4 to 7. Endocardial borders for each ventricle were semi-automatically identified using a level-set algorithm within a custom MATLAB program (The Mathworks, Natick, MA, USA) (*Figure 1B*). Circumferential strain vs. time curves for 12 segments around each ventricle in each short-axis image was generated using a custom displacement-based feature-tracking algorithm applied to the endocardial borders (*Figure 1C* and *D*). Briefly, a spatially smooth boundary displacement field (*Figure 1E*) was derived based on image similarity using a normalized cross-correlation function. Twelve evenly spaced nodes around the boundary were then specified on the first frame (*Figure 1C*) and propagated throughout all frames using the boundary displacements. Inter-node distances were adjusted to avoid an unrealistic 'jump' of the nodes, followed by temporal smoothing with a Gaussian filter. Finally, the circumferential strain curve for each segment was computed as the change in the segmental length relative to the first frame. Supplementary data online, *Appendix* (13 June 2004, date last accessed). provides details of the custom feature-tracking method. To assess inter-observer variability, CMR images from 10 patients were randomly selected and analysed independently by a second research assistant.

Quantification of dyssynchrony

To quantify the timing of contraction for each segment throughout the heart, a patient-specific reference strain vs. time curve was derived from the LV of each subject using a QT-clustering method as described previously.[7] The temporal offset (TO, in ms) relative to the LV reference curve was calculated for each of the segmental strain curves in both ventricles (*Figure 2A* and *B*). The TOs were mapped onto a bullseye and then smoothed spatially with a cubic spline (*Figure 2C*).

The intra-ventricular dyssynchrony index (DI) for the LV and RV was defined as the standard deviation (SD) of the TOs (*Figure 2D*). The inter-ventricular DI was calculated as the difference between the median LV TO and median RV TO (*Figure 2D*). To further investigate regional dyssynchrony, we calculated the median TOs separately for the following regions: RV outflow tract (RVOT), sinus and septum of the RV, and infero-lateral wall, antero-lateral wall and septum of the LV.

Statistics

All statistical analyses were performed in MATLAB. All parameters measured in the current study were normally distributed. Differences in the three DIs between patients and controls were evaluated with a two-tailed unpaired Student's *t*-test. A two-way ANOVA with Tukey *post hoc* test was used to compare regional dyssynchrony data. Inter-test and inter-observer reproducibility was assessed using Bland–Altman plots, coefficients of variation (CoVs), and intra-class correlation coefficients (ICCs). The CoV was calculated as the SD of the inter-test/inter-observer differences divided by the mean. Correlations between the DIs and electrocardiographic/functional measures were analysed using Pearson's correlation and linear regression. *P*-values of <0.05 were considered statistically significant. Results are reported as means ± SD.

Results

Study subjects

Table 1 provides basic characteristics of the study population. Patients with rTOF had various types of surgeries including transannular patch repair ($n = 19$), RV to pulmonary artery conduit ($n = 5$), and valve-sparing repair ($n = 6$). Three patients underwent subsequent pulmonary valve replacement and no patients had residual pulmonic stenosis. Most patients had significant pulmonary regurgitation (mean regurgitant fraction = 31 ± 18%).

Volumes, mass, and EF

Table 2 summarizes that the patients had normal LV volumes and EF with decreased LV mass compared with the controls. The patients also had a dilated RV with increased volumes and normal EF and mass.

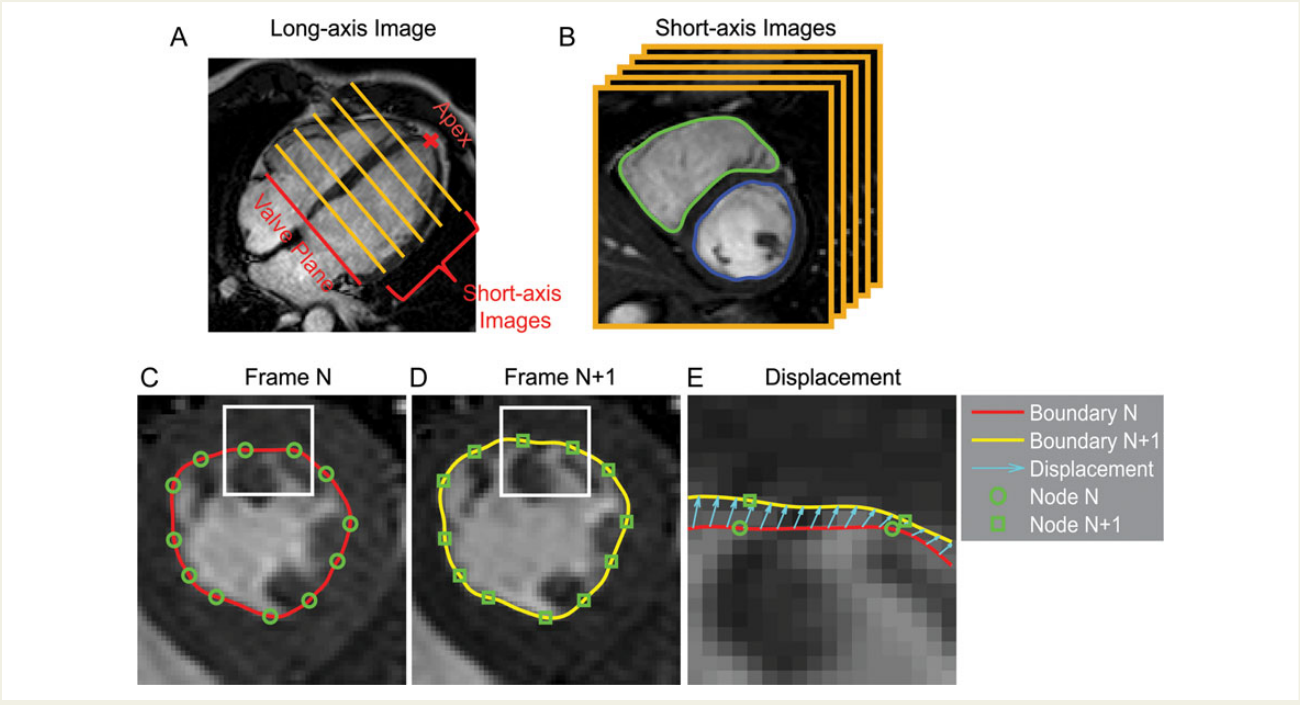

Figure 1: Illustration of the endocardial feature-tracking algorithm. Short-axis images from the apex to the valve plane were selected for processing (*A*) and endocardial boundaries were semi-automatically defined (*B*). Twelve nodes were defined on the first image frame (*C*) and were tracked to the next image frame (*D*) using the displacement field that was computed based on local changes in the image intensity patterns (*E*).

Electrocardiogram

The controls had normal ECG as required during enrolment. All patients were in normal sinus rhythm and no arrhythmia was observed. Most patients (93%) had RBBB ($n = 25$), while two patients had incomplete RBBB and one patient had left bundle branch block (LBBB). Most patients (87%) had a prolonged QRS duration of >120 ms. The mean QRS duration was prolonged in the patients compared with the controls (150 $\pm$ 27 vs. 85 $\pm$ 8 ms, $P < 0.001$).

Intra-ventricular dyssynchrony

An example of LV and RV segmental circumferential strain curves for patients and controls is shown in *Figure 3*. Results for all DIs are shown in *Figure 4* and *Table 3*. Patients with rTOF had a greater LV DI (21 $\pm$ 8 vs. 11 $\pm$ 5 ms, $P < 0.001$, *Figure 4A*) and RV DI (60 $\pm$ 19 vs. 47 $\pm$ 17 ms, $P = 0.02$, *Figure 4B*) compared with controls. The RV DI was generally larger than the LV DI for both patients and controls (compare *Figure 4B* with *Figure 4A*).

Inter-ventricular dyssynchrony

Patients had a greater inter-ventricular DI with the RV contracting 45 $\pm$ 25 ms later than the LV vs. 12 $\pm$ 29 ms earlier in controls ($P < 0.001$, *Figure 4C*). This large inter-ventricular dyssynchrony in the patients was due to the globally delayed RV contraction in the patients (*Figure 5*). *Figure 5* shows that the global median LV and RV TOs were both close to 0 in controls. However, in patients, the median LV TO was close to 0, but the median RV TO was significantly delayed. These results are also summarized in *Table 3*.

Regional dyssynchrony and pattern of contraction

Median TOs in different regions of the ventricle are shown in *Figure 5*, and the average TOs of patients and controls were mapped onto a bullseye for visualization (*Figure 6*). The normal LV had the most synchronous contraction (*Figures 5B* and *6B*). Compared with the controls, patients had earlier LV septal contraction and delayed contraction in the LV infero-lateral wall (*Figures 5B* and *6D*). The patients also had delayed contraction in all RV regions (*Figures 5C* and *6C*). Contraction patterns in the RV between controls and patients were distinct: in controls, contraction occurred in the RVOT first, followed by the sinus and septum (*Figures 5C* and *6A*); while in patients (*Figures 5C* and *6C*), the order was septum, sinus, and then RVOT.

Inter-test and inter-observer reproducibility

The LV and inter-ventricular DIs had acceptable inter-test reproducibility with CoVs ~15% and ICC $\geq$0.7 (*Table 4* and *Figure 7*). Importantly, the magnitude of the observed differences between patients and controls for the LV and inter-ventricular DIs was larger than the estimated inter-test reproducibility (i.e. the difference between patients and controls fell outside the 95% Bland–Altman limits derived from the two tests). The RV DI showed less optimal reproducibility (CoV = 22% and ICC = 0.43). All DIs showed excellent inter-observer reproducibility with CoVs <10% and ICC $\geq$0.76 (*Table 4* and *Figure 7*).

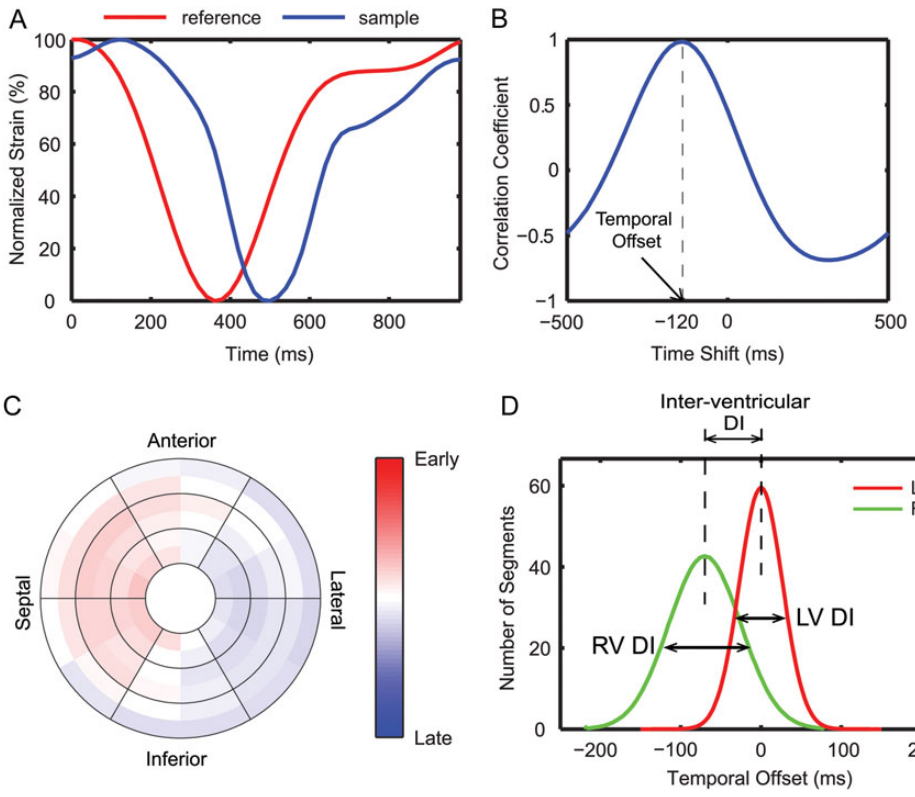

Figure 2: Quantification of dyssynchrony from circumferential strain curves. (*A*) An example of a segmental strain curve (blue) compared with the patient-specific reference curve (red). (*B*) Cross-correlation analysis was used to derive the TO for each segment. (*C*) The LV TOs from a representative patient are colour coded on a bullseye (red: early contraction; blue: late contraction; white: synchronous contraction compared with the reference curve). (*D*) A schematic showing the distribution of TOs in the LV and RV and definition of DIs.

Correlation of dyssynchrony with QRS duration, EF, mass, and volumes

QRS duration was correlated with LV DI, but not RV or inter-ventricular DI in patients with rTOF (*Table 5*). Most of the parameters of LV function were correlated with the LV and RV DI (*Figure 8*). However, correlations between RV functional parameters and DIs were mostly non-significant. Inter-ventricular DI was not correlated with any of the parameters except RV ESV.

Discussion

We implemented a custom CMR feature-tracking algorithm to show that (i) patients with rTOF suffer from left, right, and inter-ventricular cardiac dyssynchrony and (ii) the degree of dyssynchrony in both the left and right ventricles was in general correlated with measures of left ventricular but *not* right ventricular function. To our knowledge, this is the most comprehensive study to date examining dyssynchrony throughout the heart in patients with TOF. This new approach can ultimately lead to a better and more comprehensive understanding of the role of dyssynchrony in the development of ventricular dysfunction after surgical repair of TOF.

Causes of ventricular dysfunction in patients with rTOF

Patients with rTOF often develop ventricular dysfunction as they age. Understanding the causes of this dysfunction is critical to developing new therapies and reducing the late mortality in this growing patient population.[2] Cardiac dyssynchrony may play a role in causing dysfunction in patients with rTOF due to the fact that (i) surgical repair of TOF causes prolonged QRS duration with RBBB in the majority of patients[8] and (ii) QRS duration is a strong predictor of mortality in patients with rTOF.[9]

We found that the degree of dyssynchrony in both the LV and RV was in general correlated with measures of LV, but not RV, function. Consistent with this finding, Tzemos *et al.*[10] reported a correlation between LV EF and LV dyssynchrony in patients with rTOF. This raises important questions about the contribution of dyssynchrony to the longitudinal development of ventricular dysfunction in patients with rTOF, and future studies can now apply this methodology to more directly study this relationship. The lack of correlation between dyssynchrony and RV function is contradictory to other studies.[11] This could be due to the fact that we evaluated dyssynchrony in a more comprehensive way in ~100 regions compared with 2–4 regions in previous studies. However, the exact reason for this discrepancy is not clear and could be elucidated in future studies.

Dyssynchrony in patients with rTOF

Several studies have reported LV, RV, and inter-ventricular dyssynchrony in patients with rTOF using echocardiography.[3,10–16] In agreement with these studies, our data showed a significantly elevated LV DI, RV DI, and an inter-ventricular dyssynchrony mediated through a global delay in RV contraction. The LV dyssynchrony may be attributed to ventricular–ventricular interaction[17] and may help explain why LV failure develops in some patients with rTOF.[10]

Table 1 Demographic and electrocardiographic data in controls and patients with rTOF

Variable	Controls ($n = 17$)	Patients ($n = 30$)	*P*-value
Age at CMR	29 ± 7	28 ± 16	0.78
Male/female	15/2	16/14	0.001
Age at complete repair (years)	N/A	4 ± 7[a]	
Body surface area (m^2)	1.86 ± 0.17	1.79 ± 0.33	0.41
PR fraction (%)	N/A	31 ± 18	
RR interval (ms)	946 ± 117	866 ± 107	0.02
QRS duration (ms)	85 ± 8[b]	150 ± 27	<0.001
Normal sinus rhythm	100%	100%	1
Conduction block			
RBBB	0%	83%	0.004
Incomplete RBBB	0%	7%	
LBBB	0%	3%	
None	100%	7%	

CMR, cardiac magnetic resonance; PR, pulmonary regurgitation.
[a]Age at complete repair was available for 25 of the 30 patients.
[b]Note that QRS data are reported from 13 of the 17 normal subjects as the ECGs for the other four subjects were read normal by a cardiologist on enrolment, but subsequently could not be recovered.

The inter-ventricular dyssynchrony is likely associated with RBBB, but pulmonary regurgitation and RV volume overload are also possible contributors.[11] Compared with previous studies, we comprehensively analysed dyssynchrony using a hundred small segments in contrast to 2–4 regions throughout both ventricles, and observed distinct contraction patterns in the RV between patients and controls. This highlights the importance of analysing the actual pattern of contraction in addition to looking at global measures of dyssynchrony.

In the current study, we analysed septal strains from the endocardial surfaces of both the LV and RV sides of the septum. Our results show that the median TOs of the LV and RV septal regions differed by 40 ms (+10 ms for the LV and −30 ms for the RV, *Figure 5*), which is likely due to the conduction block (RBBB) in the RV septum caused by the surgical repair. Also, peak strains were lower on the RV septum compared with the LV (*Figure 3*). This could be attributed to a transmural gradient in strain across the septum, or the presence of shear strain within the septum. Future studies using advanced imaging techniques with the ability to determine strain patterns with high resolution within the septum, such as cine Displacement ENcoding with Stimulated Echoes (DENSE), may help explain these findings.[18]

Normal pattern of right ventricular contraction

The RV has traditionally been very difficult to image and understand due to its complex, non-circular geometry and thin walls. Thus, the sequence of contraction in the normal RV is not very well understood, with conflicting evidence in the literature. For example, two studies reported that regions near the RVOT are the earliest to contract,[19,20] which is similar to our findings. However, others have shown either the apex[21] or inflow regions[22] contract first. Future studies with improved, higher resolution imaging focused on quantification of RV contraction will likely play an important role in not only resolving this discrepancy, but also in understanding pathological patterns of contraction in the setting of heart disease.

Table 2 Functional data in controls and patients with rTOF

	Absolute measurements			Indexed to body surface area ($/m^2$)		
	Controls ($n = 17$)	Patients ($n = 30$)	*P*-value	Controls ($n = 17$)	Patients ($n = 30$)	*P*-value
Left ventricle						
Mass (g)	116 ± 25	88 ± 34	0.004	62 ± 9	48 ± 12	<0.001
End-diastolic volume (mL)	174 ± 27	158 ± 48	0.20	93 ± 10	88 ± 16	0.18
End-systolic volume (mL)	72 ± 15	69 ± 30	0.71	39 ± 7	38 ± 12	0.87
Stroke volume (mL)	103 ± 22	89 ± 23	0.06	55 ± 10	50 ± 8	0.05
EF (%)	59 ± 7	57 ± 6	0.45	N/A	N/A	N/A
Right ventricle						
Mass (g)	53 ± 16	49 ± 13	0.35	28 ± 5	27 ± 6	0.68
End-diastolic volume (mL)	200 ± 32	254 ± 69	0.003	107 ± 13	143 ± 35	<0.001
End-systolic volume (mL)	102 ± 19	136 ± 46	0.005	54 ± 8	76 ± 22	<0.001
Stroke volume (mL)	97 ± 19	118 ± 34	0.02	52 ± 9	67 ± 19	0.004
EF (%)	49 ± 5	47 ± 8	0.37	N/A	N/A	N/A

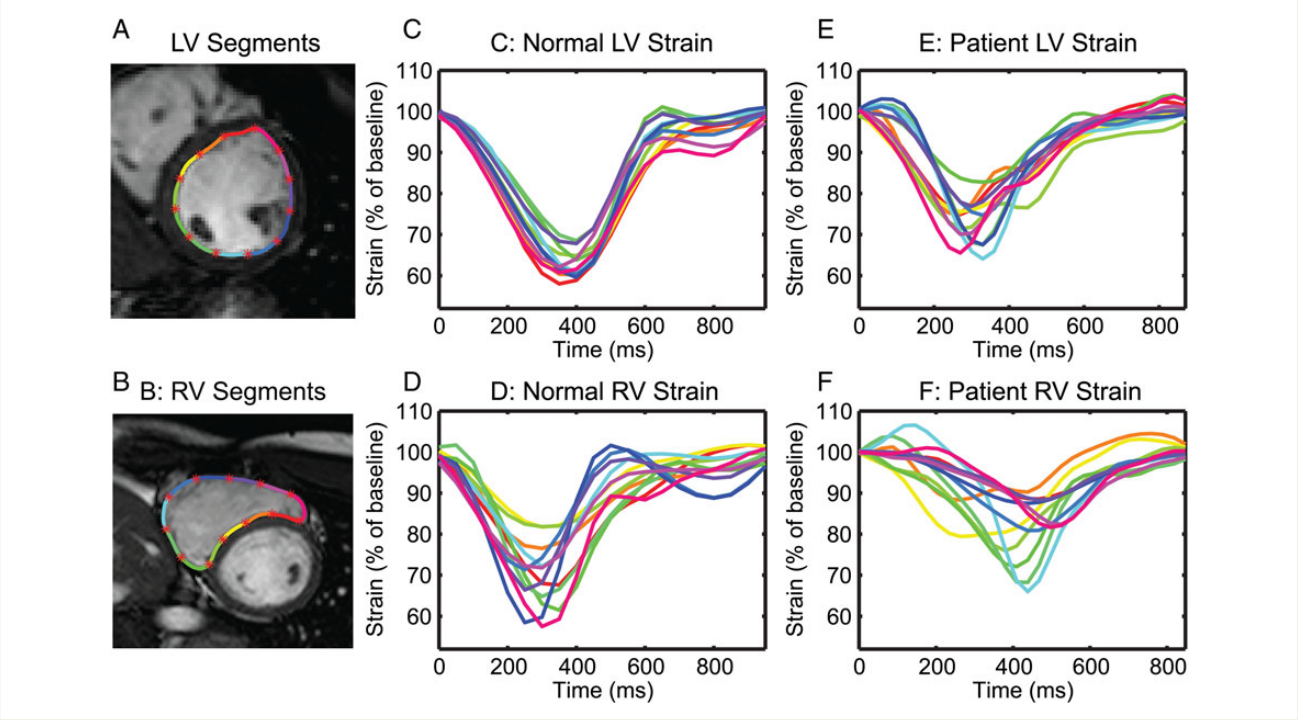

Figure 3: Representative LV (*A*) and RV (*B*) circumferential segments with corresponding strain curves. Note that the normal LV (*C*) has the most synchronous contraction with all strain curves peaking at roughly the same time, while the patient LV (*E*) exhibits a less coordinated contraction. Strain curves from the RV segments are less synchronous compared with the LV in both controls (*D*) and patients (*F*). Also note that the timing of contraction in the patient RV (*F*) occurs later in the cardiac cycle compared with the control (*D*).

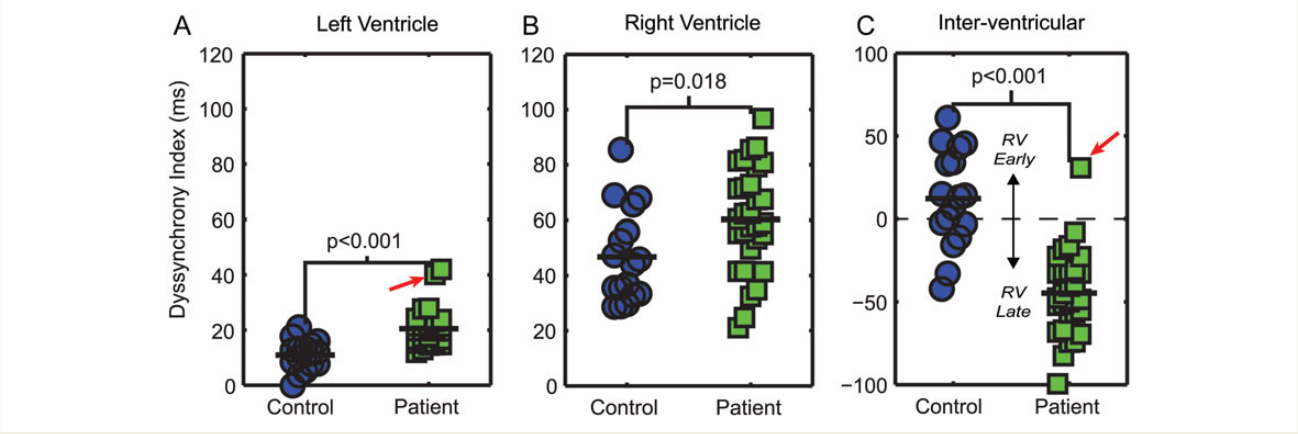

Figure 4: Patients with rTOF ($n = 30$) have elevated left (*A*), right (*B*), and inter-ventricular (*C*) DIs compared with controls ($n = 17$). Note that for the inter-ventricular DI, positive values represent early RV contraction, whereas negative values correspond to delayed RV contraction. The outlier (red arrow) is the only patient with LBBB.

Correlation of dyssynchrony with QRS duration

Our data showed prolonged QRS with a conduction block in patients with rTOF, consistent with the literature[3,10,16] and likely a result of surgical repair.[8] It is important to note that QRS duration was weakly correlated with LV dyssynchrony and not correlated with RV or inter-ventricular dyssynchrony in our study. Although prolonged QRS duration usually suggests delayed electrical activation (electrical dyssynchrony), which could further lead to mechanical dyssynchrony, studies have shown that total electrical activation time does not necessarily correlate with QRS duration.[23] Thus, our results suggest that dyssynchrony may be an independent indicator for adverse ventricular function and outcome.

Abnormal electrical activation of the ventricles in patients with rTOF has been documented previously.[24] Noticeably, the mechanical contraction pattern observed in the current study coincides with the reported electrical activation: compared with the LV, activation is delayed in the whole RV, with the latest activation at the base near RVOT. This agreement could potentially be explained by the underlying electromechanical coupling throughout the ventricle,[25] which further indicate RBBB as a potential contributor to the observed mechanical dyssynchrony.

Table 3 Summary of the DIs

DIs (ms)	Controls ($n = 17$)	Patients ($n = 30$)	*P*-value
LV DI	11 ± 5	21 ± 8	<0.001
RV DI	47 ± 17	60 ± 19	0.02
Inter-ventricular DI	12 ± 29	− 45 ± 25	<0.001
LV median TO	0 ± 1	0 ± 3	0.93
RV median TO	12 ± 29	− 45 ± 23	<0.001

Inter-test reproducibility

Our technique had acceptable inter-test reproducibility for LV and inter-ventricular DI. Although the reproducibility of the RV DI was not optimal, the CoV and ICC values were still comparable with a previous study.[26] To our knowledge, no other study has measured the inter-test reproducibility of dyssynchrony in patients with rTOF. We believe that the relatively lower reproducibility of the RV DI was primarily due to variability in the slice locations and orientations between the two scans. Future studies can investigate this and may be able to overcome this limitation using fully 3D techniques. Nonetheless, variations between patients in the different types of dyssynchrony suggest that individual measurements, not only group averages, may also be informative and important in understanding the pathophysiology of cardiac dyssynchrony in patients with rTOF.

Quantification of dyssynchrony using cine SSFP CMR

In the current study, we utilized a custom endocardial feature-tracking algorithm to quantify dyssynchrony throughout the heart, which we believe has several advantages. First, the RV is easily visualized in CMR with no limitations to imaging planes (which is an inherent problem with echocardiography). This enables interrogation of roughly 100 segments throughout the heart to provide a comprehensive understanding

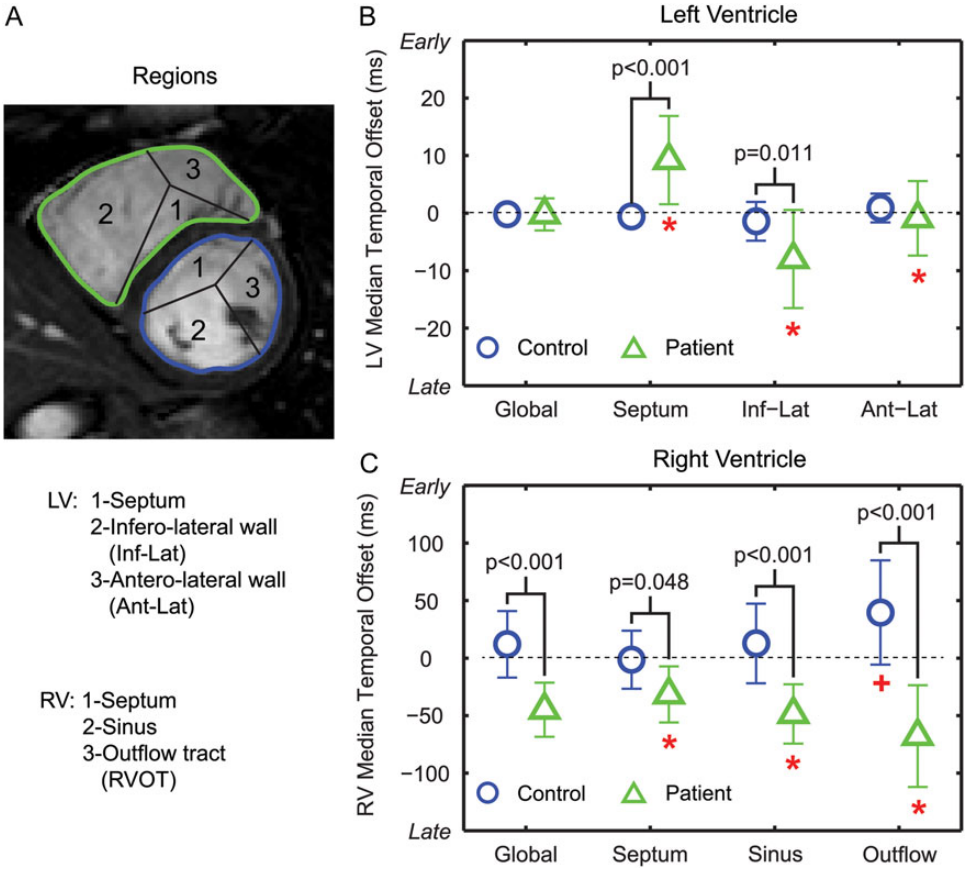

Figure 5: Global and regional median TOs in the LV (*B*) and RV (*C*) in patients and controls. *$P < 0.05$ between the three LV/RV regions (*A*) in patients. $^{+}P < 0.05$ between RVOT and the other two RV regions in controls.

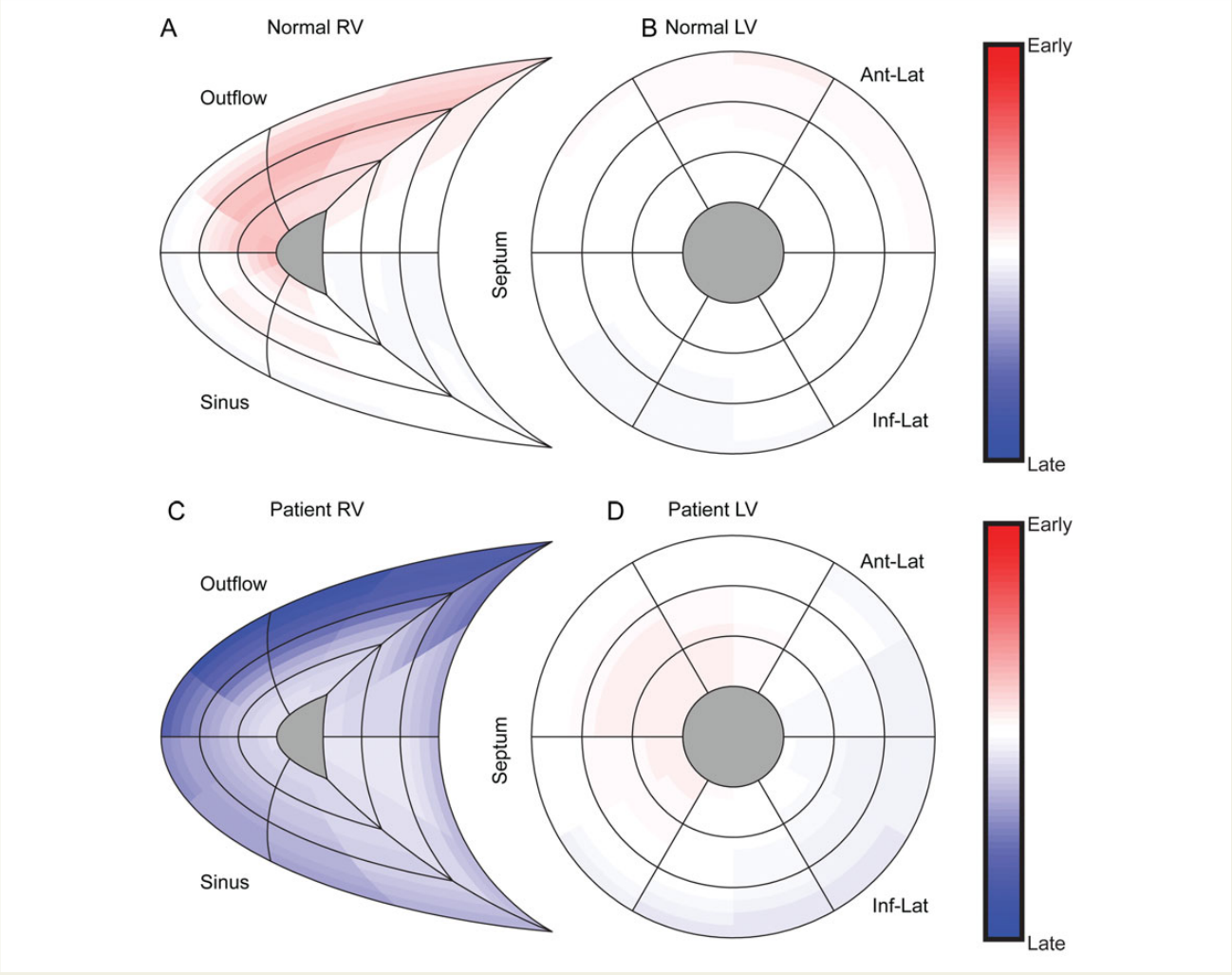

Figure 6: Average TOs of controls (*A* and *B*, $n = 17$) and patients with rTOF (*C* and *D*, $n = 30$) mapped onto a bullseye. The TOs are colour coded from red ($\geq$200 ms earlier than the reference curve) to blue ($\geq$200 ms later than the reference curve).

Table 4 Inter-test and inter-observer reproducibility for DIs in patients with rTOF[a]

DIs (ms)	Test 1	Test 2	Mean diff ± SD	CoV	ICC (95% CI)
Inter-test					
LV DI	21 ± 7	20 ± 8	0 ± 5	14%	0.70 (0.46–0.84)
RV DI	59 ± 24	62 ± 21	6 ± 24	22%	0.43 (0.10–0.68)
Inter-ventricular DI	−44 ± 25	−46 ± 27	−3 ± 11	16%	0.91 (0.82–0.96)
DIs (ms)	**Obs 1**	**Obs 2**	**Mean diff ± SD**	**CoV**	**ICC (95% CI)**
Inter-observer					
LV DI	21 ± 4	21 ± 6	0 ± 4	9%	0.76 (0.32–0.93)
RV DI	60 ± 15	60 ± 17	0 ± 10	9%	0.84 (0.51–0.96)
Inter-ventricular DI	−50 ± 17	−53 ± 16	4 ± 7	7%	0.90 (0.66–0.97)

Mean Diff, mean difference between two tests; CI, confidence interval; Obs, observer.
[a]Note that only 18 of the 30 patients were used to prospectively quantify the inter-test reproducibility of the DIs since the first 12 were randomly selected and used to optimize the methodology. Inter-observer reproducibility was assessed in 10 of the 30 patients.

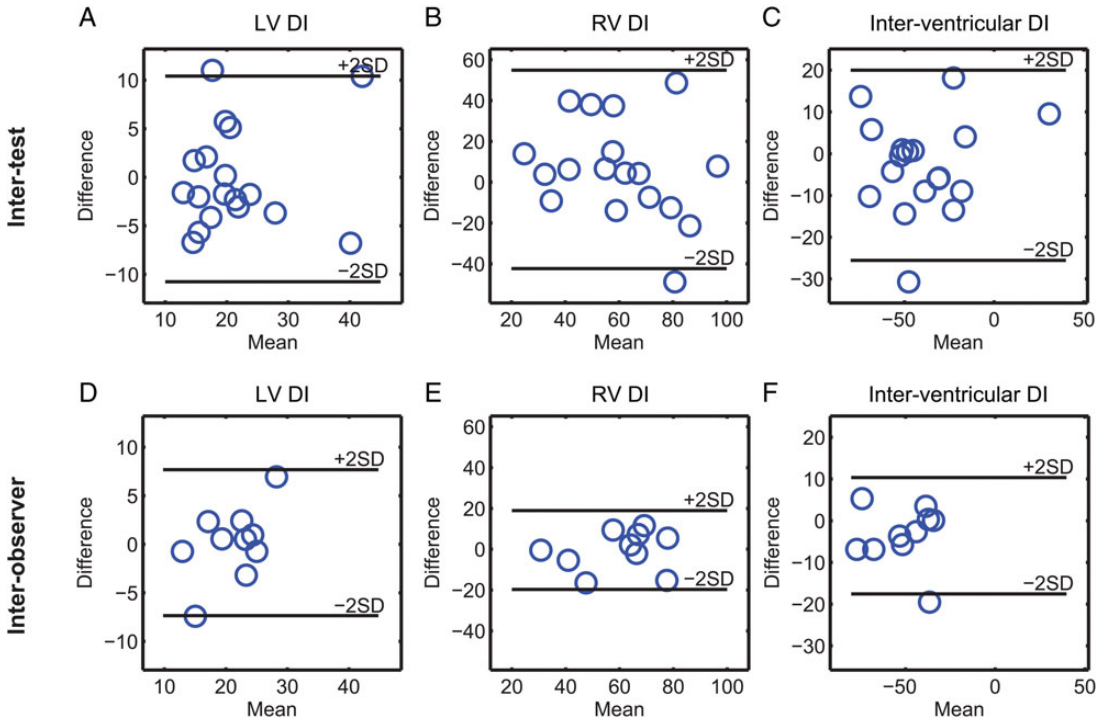

Figure 7: All DIs show good to acceptable inter-test (*A*–*C*, $n = 18$) and excellent inter-observer (*D*–*F*, $n = 10$) reproducibility in patients with rTOF. Note that inter-test reproducibility is limited to 18 patients since the first 12 patients were randomly selected and used to optimize the methodology. Inter-observer analysis is reported in 10 patients.

Table 5 Correlation of DIs with QRS duration, EF, mass, and volumes in patients with rTOF ($n = 30$)

	LV DI		RV DI		Inter-ventricular DI	
	R	*P*-value	*R*	*P*-value	*R*	*P*-value
QRS duration	0.41	0.02	0.13	0.49	−0.31	0.09
LV EDV	0.71	<0.001	0.54	0.002	0.19	0.31
LV ESV	0.79	<0.001	0.53	0.003	0.28	0.13
LV SV	0.46	0.01	0.43	0.02	0.04	0.85
LV EF	−0.52	0.003	−0.29	0.12	−0.28	0.13
LV mass	0.69	<0.001	0.60	<0.001	0.28	0.14
RV EDV	0.33	0.07	0.09	0.63	−0.29	0.12
RV ESV	0.41	0.02	0.18	0.35	−0.41	0.03
RV SV	0.12	0.54	−0.06	0.77	−0.03	0.87
RV EF	−0.31	0.09	−0.26	0.16	0.35	0.06
RV mass	0.44	0.02	0.38	0.04	−0.25	0.19

of the regional pattern of contraction. Secondly, the techniques we describe can be applied retrospectively to analyse cine datasets, which have been routinely acquired from patients with rTOF over the last two decades. When combined with long-term follow-up data, this provides a powerful tool for using retrospective datasets to understand the role of dyssynchrony in the development of ventricular dysfunction and mortality in patients with rTOF. Thirdly, if considering resynchronization therapy in this patient population, CMR could be used to obtain other important information to facilitate lead placement such as scar locations[27] and coronary venous anatomy.[28]

A recently developed CMR feature-tracking (FT-CMR) software (TomTec, Germany) has been reported and compared with echocardiographic speckle tracking,[29] and the inter-test reproducibility for quantifying cardiac strains has been evaluated.[26] Although we also

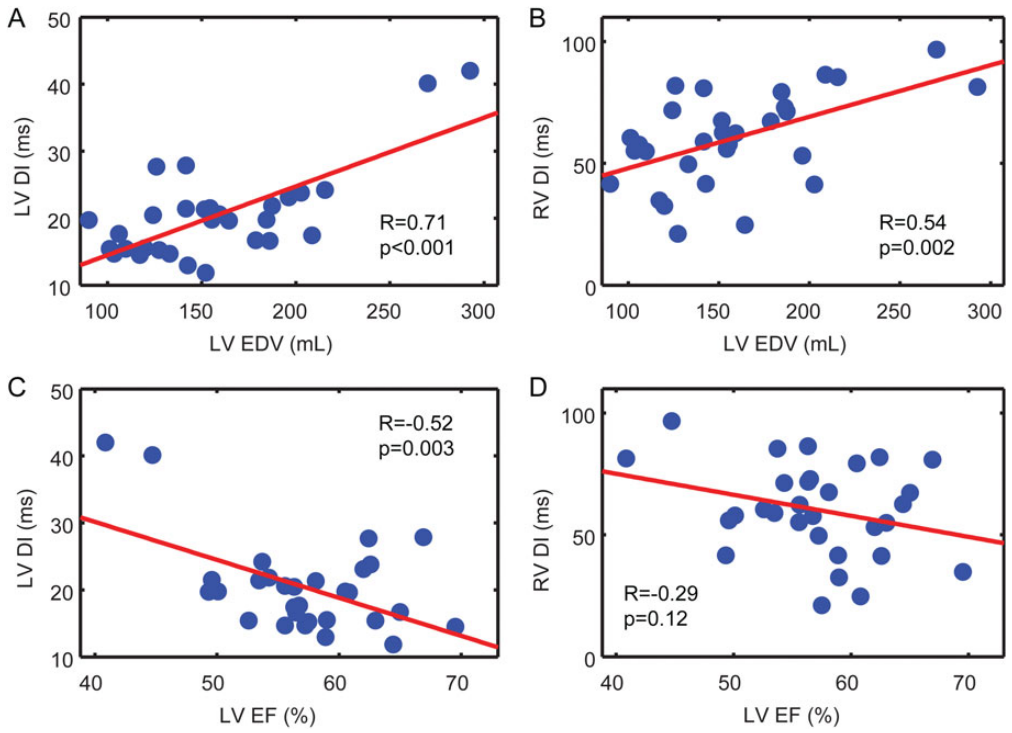

Figure 8: Correlations between measures of ventricular function and DIs. LV EDV correlated with both LV (*A*) and RV (*B*) DIs. LV EF correlated with LV DI (*C*) but not with RV DI (*D*).

used a form of feature tracking in the current study, there are several notable differences: (i) we tracked endocardial boundaries only as there are not as many features for tracking epicardial boundaries and (ii) we examined ~100 small segments throughout both ventricles, while FT-CMR has only been used to analyse strains from six regions. The inter-test CoV for our method for quantifying dyssynchrony was 14–22%, with an ICC ranging from 0.43 to 0.91. This compares favourably to reported inter-test CoVs (20–33%) and ICCs (0.44–0.7) from FT-CMR for quantifying global strains in the heart.[26] Moreover, our method had excellent inter-observer reproducibility, with CoV of 7–9% and ICC $\geq$0.76.

Limitations

Patients enrolled in the current study received different types of surgical repairs for TOF, which could have different effects on dyssynchrony. We chose not to investigate the differences among various groups, since the number of patients in each group was small. Future studies with larger patient populations will need to address this.

The male/female distribution in the control group was skewed in the current study. However, a recent study by Sun *et al.*[30] reported no gender difference in cardiac function and mechanics (twist/torsion) in healthy volunteers. Therefore, we believe that the uneven gender distribution should have minimal effects on our results.

We quantified dyssynchrony using circumferential strain curves from both ventricles, and no long-axis or RVOT views were included. This can be perceived as a limitation when analysing the RV since longitudinal motion is important to RV ejection. This may partly explain the lack of correlation between RV DI and QRS duration. However, we chose to use the short-axis slices, because these are the most widely available slices performed in routine CMR studies. Moreover, due to the fact that we utilized multiple short-axis slices and compared circumferential strains across the slices, the longitudinal component of synchrony is still incorporated and quantified by our methodology.

Strains measured by FT-CMR are derived from apparent in-plane movements, which could be attributable to through-plane displacements of obliquely orientated structures. Temporal resolution (30–50 ms) and spatial resolution (slice thickness) are also somewhat limited in standard cine CMR. In the current study, the 30–50 ms resolution is on the same magnitude of the median TO in patients. All these factors could potentially contribute to the variability in reproducibility and could be improved by more advanced MRI techniques in the future with improved spatial and temporal resolution.

We used a patient-specific reference curve derived from the LV to compute TOs for both the LV and RV. This was necessary in order to ensure a direct comparison of TOs both within and between the ventricles. In general, the shape of the RV strain curves was comparable with the LV strain curves, except in the RVOT. However, the irregular shape of the RVOT strain curves may result in unrealistic TOs using the cross-correlation method, which could increase the RV DI. Future studies may need to improve this methodology for more accurate quantification of TOs in the RVOT.

Conclusions

Patients with rTOF suffer from intra- and inter-ventricular cardiac dyssynchrony, which affect both the left and right ventricles. Endocardial feature tracking applied to cine CMR provides a potential tool to assess different types of dyssynchrony in patients with rTOF. The degree of dyssynchrony in both ventricles was in general correlated with measures of LV, but not RV, function. This new approach may be helpful in exploring the role of cardiac dyssynchrony in the longitudinal development of ventricular dysfunction in patients with rTOF.

Supplementary data

Supplementary data are available at *European Heart Journal – Cardiovascular Imaging* online.

Conflict of interest: T. G. serves as a consultant to Medtronic. The content is solely the responsibility of the authors and does not necessarily represent the official views of NIH.

Funding

This work was supported by a National Institutes of Health (NIH) Director's Early Independence Award (DP5 OD-012132), and NIH (grant number KL2 RR033171) from the National Center for Research Resources and the National Center for Advancing Translational Sciences.

References

1. Hoffman JI, Kaplan S. The incidence of congenital heart disease. *J Am Coll Cardiol* 2002; **39**:1890–900.
2. Nollert G, Fischlein T, Bouterwek S, Bohmer C, Klinner W, Reichart B. Long-term survival in patients with repair of tetralogy of Fallot: 36-year follow-up of 490 survivors of the first year after surgical repair. *J Am Coll Cardiol* 1997;**30**:1374–83.
3. Abd El Rahman MY, Hui W, Yigitbasi M, Dsebissowa F, Schubert S, Hetzer R *et al.* Detection of left ventricular asynchrony in patients with right bundle branch block after repair of tetralogy of Fallot using tissue-Doppler imaging-derived strain. *J Am Coll Cardiol* 2005;**45**:915–21.
4. van Oosterhout MF, Prinzen FW, Arts T, Schreuder JJ, Vanagt WYR, Cleutjens JPM *et al.* Asynchronous electrical activation induces asymmetrical hypertrophy of the left ventricular wall. *Circulation* 1998;**98**:588–95.
5. Fogel MA, Weinberg PM, Fellows KE, Hoffman EA. A study in ventricular-ventricular interaction. Single right ventricles compared with systemic right ventricles in a dual-chamber circulation. *Circulation* 1995;**92**:219–30.
6. Alfakih K, Plein S, Thiele H, Jones T, Ridgway JP, Sivananthan MU. Normal human left and right ventricular dimensions for MRI as assessed by turbo gradient echo and steady-state free precession imaging sequences. *J Magn Reson Imaging* 2003;**17**: 323–9.
7. Suever JD, Fornwalt BK, Neuman LR, Delfino JG, Lloyd MS, Oshinski JN. Method to create regional mechanical dyssynchrony maps from short-axis cine steady-state free-precession images. *J Magn Reson Imaging* 2014;**39**:958–65.
8. Abd El Rahman MY, Abdul-Khaliq H, Vogel M, Alexi-Meskishvili V, Gutberlet M, Lange PE. Relation between right ventricular enlargement, QRS duration, and right ventricular function in patients with tetralogy of Fallot and pulmonary regurgitation after surgical repair. *Heart* 2000;**84**:416–20.
9. Geva T. Repaired tetralogy of Fallot: the roles of cardiovascular magnetic resonance in evaluating pathophysiology and for pulmonary valve replacement decision support. *J Cardiovasc Magn Reson* 2011;**13**:9.
10. Tzemos N, Harris L, Carasso S, Dos Subira L, Greutmann M, Provost Y *et al.* Adverse left ventricular mechanics in adults with repaired tetralogy of Fallot. *Am J Cardiol* 2009;**103**:420–5.
11. Mueller M, Rentzsch A, Hoetzer K, Raedle-Hurst T, Boettler P, Stiller B *et al.* Assessment of interventricular and right-intraventricular dyssynchrony in patients with surgically repaired tetralogy of Fallot by two-dimensional speckle tracking. *Eur J Echocardiogr* 2010;**11**:786–92.
12. Bordachar P, Iriart X, Chabaneix J, Sacher F, Lafitte S, Jais P *et al.* Presence of ventricular dyssynchrony and haemodynamic impact of right ventricular pacing in adults with repaired tetralogy of Fallot and right bundle branch block. *Europace* 2008;**10**: 967–71.
13. Peng EWK, Lilley S, Knight B, Sinclair J, Lyall F, MacArthur K *et al.* Synergistic interaction between right ventricular mechanical dyssynchrony and pulmonary regurgitation determines early outcome following tetralogy of Fallot repair. *Eur J Cardiothorac Surg* 2009;**36**:694–702.
14. Thambo JB, Dos Santos P, De Guillebon M, Roubertie F, Labrousse L, Sacher F *et al.* Biventricular stimulation improves right and left ventricular function after tetralogy of Fallot repair: acute animal and clinical studies. *Heart Rhythm* 2010;**7**: 344–50.
15. Uebing A, Gibson DG, Babu-Narayan SV, Diller GP, Dimopoulos K, Goktekin O *et al.* Right ventricular mechanics and QRS duration in patients with repaired tetralogy of Fallot: implications of infundibular disease. *Circulation* 2007;**116**:1532–9.
16. Vogel M, Sponring J, Cullen S, Deanfield JE, Redington AN. Regional wall motion and abnormalities of electrical depolarization and repolarization in patients after surgical repair of tetralogy of Fallot. *Circulation* 2001;**103**:1669–73.
17. Lumens J, Ploux S, Strik M *et al.* Comparative electromechanical and hemodynamic effects of left ventricular and biventricular pacing in dyssynchronous heart failure: electrical resynchronization versus left-right ventricular interaction. *J Am Coll Cardiol* 2013;**62**:2395–403.
18. Kim D, Gilson WD, Kramer CM, Epstein FH. Myocardial tissue tracking with two-dimensional cine displacement-encoded MR imaging: development and initial evaluation. *Radiology* 2004;**230**:862–71.
19. Indik JH, Dallas WJ, Ovitt T, Wichter T, Gear K, Marcus FI. Do patients with right ventricular outflow tract ventricular arrhythmias have a normal right ventricular wall motion? A quantitative analysis compared to normal subjects. *Cardiology* 2005; **104**:10–5.
20. Matsui H, Satomi G, Yasukochi S, Kaneko S, Haseyama K. Evaluation of right ventricular contraction by myocardial strain in children using a two-dimensional tissue tracking method. *Pediatr Cardiol* 2008;**29**:377–81.
21. Atsumi A, Ishizu T, Kameda Y, Yamamoto M, Harimura Y, Machino-Ohtsuka T *et al.* Application of 3-dimensional speckle tracking imaging to the assessment of right ventricular regional deformation. *Circ J* 2013;**77**:1760–8.
22. Auger DA, Zhong XD, Epstein FH, Spottiswoode BS. Mapping right ventricular myocardial mechanics using 3D cine DENSE cardiovascular magnetic resonance. *J Cardiovasc Magn Reson* 2012;**14**:4.
23. Nanthakumar K, Masse S, Poku K, Silversides CK, Chauhan VS, Mariani JA *et al.* Intraoperative high-density global mapping in adult-repaired tetralogy of Fallot altered left ventricular and right ventricular activation and implications for resynchronization strategies. *J Am Coll Cardiol* 2010;**55**:2409–11.
24. Thambo JB, De Guillebon M, Xhaet O, Santos PD, Roubertie F, Labrousse L *et al.* Biventricular pacing in patients with tetralogy of Fallot: non-invasive epicardial mapping and clinical impact. *Int J Cardiol* 2013;**163**:170–4.
25. Russell K, Smiseth OA, Gjesdal O, Qvigstad E, Norseng PA, Sjaastad I *et al.* Mechanism of prolonged electromechanical delay in late activated myocardium during left bundle branch block. *Am J Physiol Heart Circ Physiol* 2011;**301**:H2334–43.
26. Morton G, Schuster A, Jogiya R, Kutty S, Beerbaum P, Nagel E. Inter-study reproducibility of cardiovascular magnetic resonance myocardial feature tracking. *J Cardiovasc Magn R* 2012;**14**:43.
27. Marsan NA, Westenberg JJM, Ypenburg C, van Bommel RJ, Roes S, Delgado V *et al.* Magnetic resonance imaging and response to cardiac resynchronization therapy: relative merits of left ventricular dyssynchrony and scar tissue. *Eur Heart J* 2009; **30**:2360–7.
28. Chiribiri A, Kelle S, Gotze S, Kriatselis C, Thouet T, Tangcharoen T *et al.* Visualization of the cardiac venous system using cardiac magnetic resonance. *Am J Cardiol* 2008; **101**:407–12.
29. Onishi T, Saha SK, Ludwig DR, Onishi T, Marek JJ, Cavalcante JL *et al.* Feature tracking measurement of dyssynchrony from cardiovascular magnetic resonance cine acquisitions: comparison with echocardiographic speckle tracking. *J Cardiovasc Magn Reson* 2013;**15**:95.
30. Sun JP, Lam YY, Wu CQ, Yang XS, Guo R, Kwong JS *et al.* Effect of age and gender on left ventricular rotation and twist in a large group of normal adults––a multicenter study. *Int J Cardiol* 2013;**167**:2215–21.